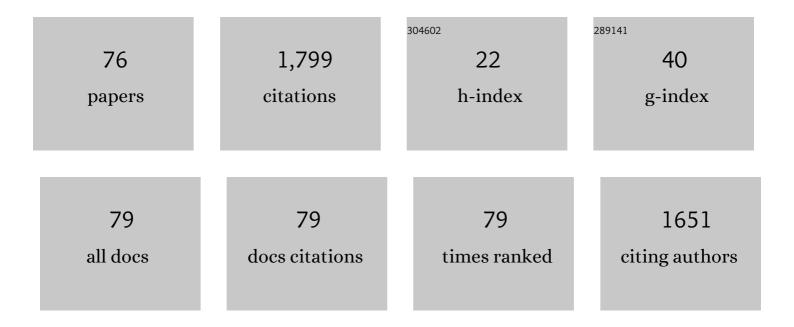
Jaeheung Park

List of Publications by Year in descending order

Source: https://exaly.com/author-pdf/3004424/publications.pdf Version: 2024-02-01



IAEHELING DADK

#	Article	IF	CITATIONS
1	The Swarm Satellite Constellation Application and Research Facility (SCARF) and Swarm data products. Earth, Planets and Space, 2013, 65, 1189-1200.	0.9	222
2	Field-aligned currents' scale analysis performed with the Swarm constellation. Geophysical Research Letters, 2015, 42, 1-8.	1.5	161
3	Comparing plasma bubble occurrence rates at CHAMP and GRACE altitudes during high and low solar activity. Annales Geophysicae, 2010, 28, 1647-1658.	0.6	104
4	Effect of sudden stratospheric warming on lunar tidal modulation of the equatorial electrojet. Journal of Geophysical Research, 2012, 117, .	3.3	81
5	Longâ€ŧerm analysis of ionospheric polar patches based on CHAMP TEC data. Radio Science, 2013, 48, 289-301.	0.8	79
6	The interhemispheric and <i>F</i> region dynamo currents revisited with the Swarm constellation. Geophysical Research Letters, 2015, 42, 3069-3075.	1.5	56
7	Scale analysis of equatorial plasma irregularities derived from Swarm constellation. Earth, Planets and Space, 2016, 68, .	0.9	51
8	Plasma blob events observed by KOMPSAT-1 and DMSP F15 in the low latitude nighttime upper ionosphere. Geophysical Research Letters, 2003, 30, .	1.5	43
9	Magnetic signatures and conjugate features of low″atitude plasma blobs as observed by the CHAMP satellite. Journal of Geophysical Research, 2008, 113, .	3.3	43
10	Climatology of the inter-hemispheric field-aligned current system in the equatorial ionosphere as observed by CHAMP. Annales Geophysicae, 2011, 29, 573-582.	0.6	43
11	Global characteristics of Pc1 magnetic pulsations during solar cycle 23 deduced from CHAMP data. Annales Geophysicae, 2013, 31, 1507-1520.	0.6	43
12	The Ionospheric Bubble Index deduced from magnetic field and plasma observations onboard Swarm. Earth, Planets and Space, 2013, 65, 1333-1344.	0.9	43
13	The characteristics of field-aligned currents associated with equatorial plasma bubbles as observed by the CHAMP satellite. Annales Geophysicae, 2009, 27, 2685-2697.	0.6	39
14	Magnetopause erosion during the 17 March 2015 magnetic storm: Combined fieldâ€aligned currents, auroral oval, and magnetopause observations. Geophysical Research Letters, 2016, 43, 2396-2404.	1.5	36
15	Characteristics of <i>F</i> â€region dynamo currents deduced from CHAMP magnetic field measurements. Journal of Geophysical Research, 2010, 115, .	3.3	35
16	The 27â€day modulation of the lowâ€latitude ionosphere during a solar maximum. Journal of Geophysical Research, 2009, 114, .	3.3	33
17	Climatology of GPS signal loss observed by Swarm satellites. Annales Geophysicae, 2018, 36, 679-693.	0.6	30
18	In-Situ CHAMP Observation of Ionosphere-Thermosphere Coupling. Space Science Reviews, 2012, 168, 237-260.	3.7	27

#	Article	IF	CITATIONS
19	Magnetic signatures of mediumâ€scale traveling ionospheric disturbances as observed by CHAMP. Journal of Geophysical Research, 2009, 114, .	3.3	25
20	Global distribution of equatorial plasma bubbles in the premidnight sector during solar maximum as observed by KOMPSAT-1 and Defense Meteorological Satellite Program F15. Journal of Geophysical Research, 2005, 110, .	3.3	24
21	Energy spectra of â^¼170–360 keV electron microbursts measured by the Korean STSAT-1. Geophysical Research Letters, 2005, 32, .	1.5	24
22	Plasma density undulations in the nighttime mid-latitude F-region as observed by CHAMP, KOMPSAT-1, and DMSP F15. Journal of Atmospheric and Solar-Terrestrial Physics, 2010, 72, 183-192.	0.6	24
23	Alfvén waves in the auroral region, their Poynting flux, and reflection coefficient as estimated from Swarm observations. Journal of Geophysical Research: Space Physics, 2017, 122, 2345-2360.	0.8	24
24	Latitude Dependence of Interhemispheric Fieldâ€Aligned Currents (IHFACs) as Observed by the Swarm Constellation. Journal of Geophysical Research: Space Physics, 2020, 125, e2019JA027694.	0.8	22
25	Daytime midlatitude plasma depletions observed by Swarm: Topside signatures of the rocket exhaust. Geophysical Research Letters, 2016, 43, 1802-1809.	1.5	21
26	Equatorial spread <i>F</i> -related currents: Three-dimensional simulations and observations. Geophysical Research Letters, 2011, 38, n/a-n/a.	1.5	20
27	Effects of sudden stratospheric warming (SSW) on the lunitidal modulation of the Fâ€region dynamo. Journal of Geophysical Research, 2012, 117, .	3.3	19
28	A dayside plasma depletion observed at midlatitudes during quiet geomagnetic conditions. Geophysical Research Letters, 2015, 42, 967-974.	1.5	19
29	Equatorial plasma bubbles with enhanced ion and electron temperatures. Journal of Geophysical Research, 2008, 113, .	3.3	18
30	Nighttime magnetic field fluctuations in the topside ionosphere at midlatitudes and their relation to mediumâ€scale traveling ionospheric disturbances: The spatial structure and scale sizes. Journal of Geophysical Research: Space Physics, 2015, 120, 6818-6830.	0.8	18
31	On the direction of the Poynting flux associated with equatorial plasma depletions as derived from <i>Swarm</i> . Geophysical Research Letters, 2017, 44, 5884-5891.	1.5	17
32	Largeâ€6cale Ducting of Pc1 Pulsations Observed by Swarm Satellites and Multiple Ground Networks. Geophysical Research Letters, 2018, 45, 12,703.	1.5	17
33	Long‣asting Latitudinal Fourâ€Peak Structure in the Nighttime Ionosphere Observed by the Swarm Constellation. Journal of Geophysical Research: Space Physics, 2019, 124, 9335-9347.	0.8	17
34	Neutral density depletions associated with equatorial plasma bubbles as observed by the CHAMP satellite. Journal of Atmospheric and Solar-Terrestrial Physics, 2010, 72, 157-163.	0.6	16
35	Global Characteristics of Electromagnetic Ion Cyclotron Waves Deduced From Swarm Satellites. Journal of Geophysical Research: Space Physics, 2018, 123, 1325-1336.	0.8	15
36	Comprehensive Analysis of the Magnetic Signatures of Small‣cale Traveling Ionospheric Disturbances,as Observed by Swarm. Journal of Geophysical Research: Space Physics, 2019, 124, 10794-10815.	0.8	15

#	Article	IF	CITATIONS
37	Morning Overshoot of Electron Temperature as Observed by the Swarm Constellation and the International Space Station. Journal of Geophysical Research: Space Physics, 2020, 125, e2019JA027299.	0.8	14
38	Morphology of highâ€latitude plasma density perturbations as deduced from the total electron content measurements onboard the Swarm constellation. Journal of Geophysical Research: Space Physics, 2017, 122, 1338-1359.	0.8	14
39	Variation of the topside ionosphere during the last solar minimum period studied with multisatellite measurements of electron density and temperature. Journal of Geophysical Research: Space Physics, 2016, 121, 7269-7286.	0.8	12
40	Periodicity in the occurrence of equatorial plasma bubbles derived from the C/NOFS observations in 2008–2012. Journal of Geophysical Research: Space Physics, 2017, 122, 1137-1145.	0.8	12
41	Plasma irregularities in the highâ€latitude ionospheric Fâ€region and their diamagnetic signatures as observed by CHAMP. Journal of Geophysical Research, 2012, 117, .	3.3	11
42	Westward tilt of low″atitude plasma blobs as observed by the Swarm constellation. Journal of Geophysical Research: Space Physics, 2015, 120, 3187-3197.	0.8	11
43	Statistical survey of nighttime midlatitude magnetic fluctuations: Their source location and Poynting flux as derived from the Swarm constellation. Journal of Geophysical Research: Space Physics, 2016, 121, 11,235.	0.8	11
44	On the Balance Between Plasma and Magnetic Pressure Across Equatorial Plasma Depletions. Journal of Geophysical Research: Space Physics, 2019, 124, 5936-5944.	0.8	11
45	Modulation of Pc1 Wave Ducting by Equatorial Plasma Bubble. Geophysical Research Letters, 2020, 47, e2020GL088054.	1.5	10
46	Ion Velocity and Temperature Variation Around Topside Nighttime Irregularities: Contrast Between Low―and Mid‣atitude Regions. Journal of Geophysical Research: Space Physics, 2021, 126, e2020JA028810.	0.8	10
47	Temporal Evolution of Lowâ€Latitude Plasma Blobs Identified From Multiple Measurements: ICON, GOLD, and Madrigal TEC. Journal of Geophysical Research: Space Physics, 2022, 127, .	0.8	10
48	Field-aligned current associated with low-latitude plasma blobs as observed by the CHAMP satellite. Annales Geophysicae, 2010, 28, 697-703.	0.6	9
49	Alfvén wave characteristics of equatorial plasma irregularities in the ionosphere derived from CHAMP observations. Frontiers in Physics, 2014, 2, .	1.0	9
50	Steepening Plasma Density Spectra in the Ionosphere: The Crucial Role Played by a Strong Eâ€Region. Journal of Geophysical Research: Space Physics, 2021, 126, e2021JA029401.	0.8	9
51	Observational Evidence for the Role of Hall Conductance in Alfvén Wave Reflection. Journal of Geophysical Research: Space Physics, 2020, 125, e2020JA028119.	0.8	9
52	Diagnosing low-/mid-latitude ionospheric currents using platform magnetometers: CryoSat-2 and GRACE-FO. Earth, Planets and Space, 2020, 72, .	0.9	9
53	Vertical Scale Height of the Topside Ionosphere Around the Korean Peninsula: Estimates from Ionosondes and the Swarm Constellation. Journal of Astronomy and Space Sciences, 2015, 32, 311-315.	0.3	9
54	Nonâ€stormtime injection of energetic particles into the slotâ€region between Earth's inner and outer electron radiation belts as observed by STSATâ€1 and NOAAâ€POES. Geophysical Research Letters, 2010, 37, .	1.5	8

#	Article	IF	CITATIONS
55	Characteristics of Ionospheric Irregularities Using GNSS Scintillation Indices Measured at Jang Bogo Station, Antarctica (74.62°S, 164.22°E). Space Weather, 2020, 18, e2020SW002536.	1.3	8
56	Statistical Analysis of Pc1 Wave Ducting Deduced From Swarm Satellites. Journal of Geophysical Research: Space Physics, 2021, 126, e2020JA029016.	0.8	8
57	Implementation of the direct locking method for long-term carrier-envelope-phase stabilization of a grating-based kHz femtosecond laser. Applied Physics B: Lasers and Optics, 2009, 96, 287-291.	1.1	7
58	Isolated Proton Aurora Driven by EMIC Pc1 Wave: PWING, Swarm, and NOAA POES Multiâ€Instrument Observations. Geophysical Research Letters, 2021, 48, e2021GL095090.	1.5	7
59	Noise features of the CHAMP vector magnetometer in the 1–25 Hz frequency range. Sensors and Actuators A: Physical, 2015, 222, 272-283.	2.0	6
60	Simultaneous Observations of SAR Arc and Its Ionospheric Response at Subauroral Conjugate Points (LÂ≃Â2.5) During the St. Patrick's Day Storm in 2015. Journal of Geophysical Research: Space Physics, 2020, 125, e2019JA027321.	0.8	6
61	Ionospheric Plasma Density Oscillation Related to EMIC Pc1 Waves. Geophysical Research Letters, 2020, 47, e2020GL089000.	1.5	5
62	Isolated Peak of Oxygen Ion Fraction in the Postâ€Noon Equatorial Fâ€Region: ICON and SAMI3/WACCMâ€X. Journal of Geophysical Research: Space Physics, 2021, 126, e2021JA029217.	0.8	5
63	FUV spectrum in the polar region during slightly disturbed geomagnetic conditions. Journal of Geophysical Research, 2011, 116, n/a-n/a.	3.3	4
64	Plasma density undulations correlated with thermospheric neutral mass density in the daytime lowâ€latitude to midlatitude topside ionosphere. Journal of Geophysical Research: Space Physics, 2015, 120, 6669-6678.	0.8	4
65	Coordinated Observations of Rocket Exhaust Depletion: GOLD, Madrigal TEC, and Multiple Lowâ€Earthâ€Orbit Satellites. Journal of Geophysical Research: Space Physics, 2022, 127, .	0.8	4
66	Exospheric Temperature Measured by NASAâ€GOLD Under Low Solar Activity: Comparison With Other Data Sets. Journal of Geophysical Research: Space Physics, 2022, 127, .	0.8	4
67	Ratio Between Overâ€Satellite Electron Content and Plasma Density Measured by Swarm: A Proxy for Topside Scale Height. Journal of Geophysical Research: Space Physics, 2022, 127, .	0.8	4
68	Hemispheric asymmetry in transition from equatorial plasma bubble to blob as deduced from 630.0Ânm airglow observations at low latitudes. Journal of Geophysical Research: Space Physics, 2016, 121, 881-893.	0.8	3
69	Ionospheric Plasma Fluctuations Induced by the NWC Very Low Frequency Signal Transmitter. Journal of Geophysical Research: Space Physics, 2021, 126, e2021JA029213.	0.8	3
70	Closure of F Region Dynamo Currents: Revisiting CHAMP Magnetic Field Data. Journal of Geophysical Research: Space Physics, 2020, 125, e2020JA028522.	0.8	2
71	Multi‥ear Statistics of LEO Energetic Electrons as Observed by the Korean NextSatâ€1. Space Weather, 2021, 19, e2021SW002787.	1.3	2
72	A Small Peak in the Swarm‣P Plasma Density Data at the Dayside Dip Equator. Journal of Geophysical Research: Space Physics, 2022, 127, .	0.8	2

#	Article	IF	CITATIONS
73	Frequency-domain performance of a femtosecond laser with carrier-envelope phase stabilized by the direct locking method. Applied Physics B: Lasers and Optics, 2011, 104, 793-797.	1.1	1
74	Coherence Scale and Directivity of Nighttime Equatorial Plasma Irregularities: Results From Swarm Formation Flight. Journal of Geophysical Research: Space Physics, 2022, 127, .	0.8	1
75	Low-latitude plasma blobs above Africa: Exploiting GOLD and multi-satellite in situ measurements. Advances in Space Research, 2023, 72, 726-740.	1.2	1
76	Full-field sub-wavelength imaging with a multiple scattering. , 2015, , .		0